



HAL
open science

Spinodal phase separation in complex fluids

F. Schmid, R. Blossey

► **To cite this version:**

F. Schmid, R. Blossey. Spinodal phase separation in complex fluids. *Journal de Physique II*, 1994, 4 (7), pp.1195-1207. 10.1051/jp2:1994194 . jpa-00248037

HAL Id: jpa-00248037

<https://hal.science/jpa-00248037>

Submitted on 4 Feb 2008

HAL is a multi-disciplinary open access archive for the deposit and dissemination of scientific research documents, whether they are published or not. The documents may come from teaching and research institutions in France or abroad, or from public or private research centers.

L'archive ouverte pluridisciplinaire **HAL**, est destinée au dépôt et à la diffusion de documents scientifiques de niveau recherche, publiés ou non, émanant des établissements d'enseignement et de recherche français ou étrangers, des laboratoires publics ou privés.

Classification

Physics Abstracts

64.70J — 64.75 — 82.70

Spinodal phase separation in complex fluids

F. Schmid ⁽¹⁾ and R. Blossey ⁽²⁾

⁽¹⁾ Department of Physics FM-15, University of Washington, Seattle WA 98195, U.S.A.

⁽²⁾ Institut für Theoretische Physik IV, Heinrich-Heine-Universität Düsseldorf, Universitätsstrasse 1, 40225 Düsseldorf, Germany

(Received 27 September 1993, revised 28 January 1994, accepted 25 March 1994)

Abstract. — We study the early stages of the phase separation of an amphiphilic system into two fluids, one structured and the other not, in the context of a one-component order-parameter model. A generalization of the Langer — Bar-on — Miller approximation permits the calculation of the time evolution of the structure function in the mixture. Near the structured-fluid side of the coexistence, we find that the spinodal is much more clearly observable and is closer to the binodal than on the unstructured side.

1. Introduction.

Phase separation occurs when a binary system (e.g. a mixture of two fluids or polymers) is quenched from a stable, homogeneous one-phase state into the two-phase region of its phase diagram [1]. The early-stage dynamics of the unmixing process has been studied first in the context of simple, mean-field like theories [2, 3]. The picture emerging from this distinguishes between two very different regimes. If the initial state right after the quench is thermodynamically metastable, phase separation must begin with the nucleation of droplets of the preferred stable phase. When the size of such a droplet exceeds a critical value, it will grow and the metastable state decays. The nucleation process itself is mediated by thermal fluctuations and is generally described in terms of the droplet nucleation rate $\Gamma \sim e^{-\varepsilon}$, where ε is the excess free energy of the critical droplet. In this first regime, phase separation is a highly inhomogeneous and stochastic process. On the other hand, phase separation from a thermodynamically unstable initial state is governed by the growth of the unstable fluctuations (spinodal decomposition). The early-stage demixing is essentially homogeneous, leading to the formation of a complex interconnected two-phase structure. In mean-field theory, both regimes are separated by a well-defined spinodal.

This simple, classical picture succeeds in qualitatively describing many experimental features of early-stage phase separation. Unfortunately, it fails as soon as fluctuations have to be included. In particular, the concept of a spinodal is generally considered to be meaningless beyond mean-field theory [1]. The main reason for this lies in the fact that the unstable

fluctuations close to the spinodal have very long wavelengths and consequently grow very slowly in time. Therefore the dominant mechanism for phase separation remains nucleation even beyond the classical spinodal. A sharp spinodal cannot be detected by experiment or by simulation.

Experimentally, the early stages of phase separation have been frequently studied in metallic alloys [4]. Unfortunately, the observation in simple binary fluids is rather difficult due to the very short time scales on which relaxation occurs. In order to circumvent this difficulty, experiments have been conducted in situations where time scales are enhanced, as is e.g. the case for quenches at the critical concentration [5]. Another strategy has been to choose experimental systems which by themselves have long relaxation times, such as polymer solutions [6, 7], equal mass solutions [8] or complex fluids such as non-ionic micellar solutions [9]. These latter systems are especially interesting because of the new effects that can be expected due to the internal structure of the homogeneous phases.

A complex fluid can exhibit disordered phases that, while being homogeneous on a microscopic scale, are internally structured. The structure shows up as a peak at non-zero wavevector in the static structure factor of scattering [10]. A prominent example of a complex fluid is the microemulsion phase in oil-water-surfactant mixtures which contains an interpenetrating network of oil-water interfaces [11]. Only recently has there been some theoretical interest in the dynamics in such systems : the relaxation after a quench into the one-phase region of the microemulsion has been studied [12] as well as the dynamics of oil-water separation in the presence of amphiphiles [13]. However, since the internal structure of a complex fluid indicates a built-in affinity towards fluctuations of a certain wavelength, it should particularly affect the spinodal decomposition in an unmixing process.

It is this question we address in the present paper. We study the early stages of phase separation into two phases, one of which is internally structured while the other is not, within a Ginzburg-Landau-type model system for a complex fluid. In particular, we are interested in the changes in the time-dependent structure factor as the average concentration is varied, and the spinodal on both the structured and the non-structured side of the phase diagram is crossed. Our approach generalizes the method of Langer, Bar-on and Miller [17] for simple binary systems, which accounts for small fluctuations. For comparison, we also study the system in mean-field theory. Our paper is organized as follows : we introduce the model in section 2 and develop the theory in section 3. Section 4 presents in detail the results for both the mean-field theory and the Langer — Bar-on — Miller — approximation. We summarize in section 5.

2. The model.

A ternary oil-water-amphiphile mixture is most naturally studied with a two-field Ginzburg-Landau functional [14],

$$\mathcal{F}[\phi, \psi] = \int d^3\mathbf{r} \{ c(\Delta\phi)^2 + g_0(\nabla\phi)^2 + W(\phi) + V(\psi, \phi) - \ell\psi(\nabla\phi)^2 \}, \quad (1)$$

where $g_0 > 0$, $c > 0$. ϕ denotes the difference between oil and water density, and ψ is the surfactant density. The last term in (1) accounts for the amphiphilic properties of the surfactant, favoring it to sit at the internal oil-water interfaces. Thus $\ell > 0$ is related to the strength of the amphiphile. $W(\phi)$ is a double-well potential with minima at the oil- and water-rich phases. Since the surfactant does not cluster and its density is small even in the microemulsion phase, we expand \mathcal{F} up to second order in ψ . We get $V(\psi, \phi) \approx v_1(\phi)\psi - \mu\psi + \frac{1}{2}v_2(\phi)\psi^2$, where $v_2(\phi) \geq 0$ for all accessible values of ϕ and μ is the chemical potential driving the surfactant density ψ .

At early times of the phase separation process, when typical length scales are still small, energy and momentum transport in the fluid are fast compared to the unmixing process. The dynamics can then be described by Langevin equations for the conserved fields ϕ and ψ . We further simplify the dynamics by assuming that the surfactant relaxes much faster than oil or water, i.e. its density follows the changes in the difference of oil and water density adiabatically. Although this last assumption is not necessarily realistic in a general experimental situation, we expect that the simplified model still contains the main characteristics of phase separation in a simple/complex-fluid mixture. We note that, the resulting model (2) being the simplest possible model with two-phase coexistence of a simple and a structured fluid, its study should give qualitative insight into the effect of internal structure on phase separation in any such system, not just in ternary mixtures.

Following our assumption, we can integrate out the field ψ quasistatically [15] which leads to an effective one-order-parameter functional [16],

$$\mathcal{F}[\phi] = \int d^3\mathbf{r} \{c(\Delta\phi)^2 + g(\phi)(\nabla\phi)^2 + f(\phi)\}, \quad (2)$$

where $g(\phi) = g_0 - \ell(\mu - v_1)/v_2$ and

$$f(\phi) = W(\phi) - (\mu - v_1)^2/2v_2 - \frac{k_B T}{2} \ln(v_2/k_B T).$$

(Higher orders in $\nabla\phi$ have been neglected in Eq. (2) as in Eq. (1)). Hence, one is left with just one equation of motion for the oil-water density ϕ

$$\partial_t \phi(\mathbf{r}, t) = \lambda \nabla^2 \frac{\delta \mathcal{F}}{\delta \phi(\mathbf{r})} + \xi(\mathbf{r}, t), \quad (3)$$

where the Gaussian white noise ξ satisfies the fluctuation-dissipation relation

$$\langle \xi(\mathbf{r}, t) \xi(\mathbf{r}', t') \rangle = -2 k_B T \lambda \nabla^2 \delta(\mathbf{r} - \mathbf{r}') \delta(t - t'). \quad (4)$$

The static properties of model (2) have been studied extensively [14] in various contexts. In mean-field theory, the homogeneous phases are given by the minima of the function $f(\phi)$. The value of $\gamma = g(\phi)/\sqrt{2cf''(\phi)}$ there determines the degree of internal structure of the fluid: for large positive values of γ the system behaves just as an ordinary fluid. At the disorder line $\gamma = 1$, correlation functions begin to show oscillatory behavior; beyond the Lifshitz line $\gamma = 0$, the structure functions exhibit a peak at nonzero q . Finally, at $\gamma = -1$, the homogeneous phase becomes unstable with respect to density fluctuations of a certain wavelength, and the lamellar phase is stable. Here we are interested in a situation at two-phase coexistence, where one has phase separation into a structured and a non-structured phase. Hence $f(\phi)$ has two minima and $g(\phi)$ is positive at one, e.g. the water rich phase, and negative at the other, e.g. the microemulsion.

3. Theory of the structure factor.

Based on the model (2), (3) we now establish the equations for the evolution in time of the structure factor. Equation (3) leads to the Fokker-Planck equation for the distribution functional $\rho[\phi; t]$,

$$\partial_t \rho = - \int d^3\mathbf{r} \frac{\delta^2 \rho[\phi; t]}{\delta \phi(\mathbf{r})^2} \quad (5)$$

with the probability current

$$\partial_t [\phi ; t] = \lambda \nabla^2 \left[\Pi(\mathbf{r}) \cdot \rho + k_B T \frac{\delta \rho}{\delta \phi(\mathbf{r})} \right], \quad (6)$$

where

$$\Pi(\mathbf{r}) = \frac{\delta \mathcal{F}}{\delta \phi(\mathbf{r})} = 2c \Delta^2 \phi - 2g \Delta \phi - \frac{\partial}{\partial \phi} g(\nabla \phi)^2 + \frac{\partial}{\partial \phi} f. \quad (7)$$

From (5) we find that the structure factor, $\hat{S}(\mathbf{k}) \equiv \langle \hat{\phi}(\mathbf{k}) \hat{\phi}(-\mathbf{k}) \rangle$, obeys

$$\partial_t \hat{S}(\mathbf{k}) = -\lambda k^2 [\langle \hat{\Pi}(\mathbf{k}) \hat{\phi}(-\mathbf{k}) \rangle + \langle \hat{\Pi}(-\mathbf{k}) \hat{\phi}(\mathbf{k}) \rangle] + 2\lambda k_B T k^2, \quad (8)$$

where $\hat{\cdot}$ indicates a Fourier transform and the brackets $\langle \dots \rangle$ denote the average with respect to the joint probability functional $\rho[\hat{\phi}; t]$.

In order to solve these equations, we adopt the route taken by Langer, Bar-on and Miller [17], and factorize ρ in a convenient way: let $\rho^{(n)}$ denote the n -point distribution function

$$\rho_{\mathbf{r}_1, \dots, \mathbf{r}_n}^{(n)}(u_1, \dots, u_n) = \langle \delta(u(\mathbf{r}_1) - u_1) \dots \delta(u(\mathbf{r}_n) - u_n) \rangle,$$

where $u(\mathbf{r}) = \phi(\mathbf{r}) - \langle \phi \rangle$ are the fluctuations in the field $\phi(\mathbf{r})$. We expand the expression $\rho^{(n)}(u_1, \dots, u_n) / [\prod_{i=1}^n \rho^{(1)}(u_i)]$ up to second order in the u_i and obtain

$$\rho_{\mathbf{r}_1, \dots, \mathbf{r}_n}^{(n)}(u_1, \dots, u_n) = \left[\prod_{i=1}^n \rho^{(1)}(u_i) \right] \left[1 + \sum_{i < j} \gamma(\mathbf{r}_i, \mathbf{r}_j) u_i u_j \right]. \quad (9)$$

Here γ is related to the structure function by $\gamma(\mathbf{r}_i, \mathbf{r}_j) \langle u^2 \rangle^2 = S(\mathbf{r}_i - \mathbf{r}_j)$. For $n=2$ equation (9) recovers the ansatz for the two-point distribution functional $\rho^{(2)}$ used by Langer *et al.* However, as opposed to the model for simple binary mixtures treated there, the right hand side of equation (8) involves also three-point correlations functions.

With the ansatz (8) and (9), the time derivative of the structure function $\partial_t \hat{S}(\mathbf{k})$ can be expressed as a function of $\hat{S}(\mathbf{k})$ and $\rho^{(1)}$ alone. Using equations (5) and (6), we find

$$\partial_t \rho^{(1)}(u) = \lambda \sum_{\mathbf{k}} k^2 e^{-i\mathbf{k} \cdot \mathbf{r}} \left\langle \left[\hat{\Pi}(\mathbf{k}) \frac{\partial}{\partial u} + k_B T \frac{\partial^2}{\partial u^2} \right] \delta(\phi(\mathbf{r}) - u) \right\rangle, \quad (10)$$

which also involves only the structure function and $\rho^{(1)}$. Thus, the set of equations (8) and (10) is closed. They will be solved numerically in the following section. In practice we use the potential $\frac{1}{k_B T} f(\phi) = \frac{1}{4} (\phi^2 - 1)^2$ and assume $\frac{1}{k_B T} g(\phi) = -\bar{g}\phi$, so that g is negative for

positive ϕ and positive for negative ϕ . Furthermore, we fix $\frac{1}{k_B T} c = 1$ and $k_B T \lambda = 1$ thus setting the units of time and space. In the complex fluid phase, the equilibrium structure function $\hat{S}(\mathbf{k})$ has a maximum at $\mathbf{k} = \sqrt{\bar{g}/2} c = 0.92$ at $\bar{g} = 1.7$.

Since the final result is rather technical, we relegate it to the appendix and conclude this section with a few comments on the validity of the approximation (9). Technically, the calculation breaks down as soon as the higher moments $\langle u^n \rangle$ of the fluctuation field become too large compared to the first ones. The fluctuations u obviously have to be small, since equation (9) is an expansion in u . This limits the applicability of our approach to early times. A

more serious shortcoming of equation (9) is that it does not include effects of inhomogeneities and assumes correlations to be independent of whether fluctuations occur in the same or different domains. Therefore, the approximation will not be able to treat phase separation correctly wherever nucleation effects are important. In the spinodal regime, however, the system decomposes homogeneously and our treatment will provide an appropriate description.

4. Results.

Having established the basic equations, we are now ready to present the results for the structure function. To begin with, we discuss the Gaussian approximation, in which only the leading order in the fluctuations u is kept in equation (15) and (16). The structure function is found to obey the equation

$$\partial_t \hat{S}(\mathbf{k}) = -2 \lambda k^2 \hat{S}(\mathbf{k}) A(\mathbf{k}) + 2 \lambda k_B T k^2 \quad (11)$$

with

$$A(\mathbf{k}) = 2 c k^4 + 2 k^2 g(\phi) + f''(\phi). \quad (12)$$

Equations (11) and (12) correspond to the Cahn-Hilliard-Cook approximation for the structure factor [2, 18]. Within this approximation, fluctuation modes with different wavevectors decouple and each relaxes exponentially with its own characteristic time $1/\tau(\mathbf{k}) = 2 \lambda k^2 A(\mathbf{k})$. The mode becomes unstable when $\tau(\mathbf{k})$ becomes negative. Suppose now that the quench experiment starts at some homogeneous concentration ϕ_0 and then the system is brought rapidly into the coexistence region. If $\tau(\mathbf{k})$ is positive for all \mathbf{k} , the system reaches a metastable homogeneous state after some time, which can only decay by nucleation processes for which there is no mechanism in the theory we use.

As soon as τ becomes negative for some \mathbf{k} , the corresponding mode grows exponentially and initiates the unmixing process. In a simple binary fluid where $g > 0$, the classical spinodal that separates the nucleation and spinodal decomposition regimes is given by $f''(\phi_0) = 0$. The maximum growth rate $\omega_p = \max_{\mathbf{k}} [-1/\tau(\mathbf{k})]$ drops to zero with vanishing slope as the spinodal

is approached (Fig. 1a, $\phi < 0$ and $g(\phi) \propto -\bar{g}\phi$) and the unstable modes are those with small wavevector \mathbf{k} (Fig. 1b, $\phi < 0$). Therefore, unstable modes grow very slowly close to the spinodal and will never provide the dominant mechanism for phase separation. As discussed in the Introduction, this implies that in practice the nucleation and the spinodal decomposition regimes cannot clearly be separated and the spinodal is meaningless.

The situation is different in a complex fluid with $g < 0$. Here, modes with finite wavevector $\mathbf{k}^2 = -g(\phi_0)/2c$ become unstable before the ordinary spinodal is reached. Spinodal decomposition occurs as soon as

$$f''(\phi_0) \leq g(\phi_0)^2/2c \quad (13)$$

is fulfilled. The consequences are illustrated in figures 1a and 1b. Compared to the simple fluid side at $\phi_0 < 0$, two important changes occur on the complex fluid side ($\phi_0 > 0$). First, the spinodal is shifted towards the binodal at $\phi = 1$, the region of spinodal decomposition is enlarged. In the extreme case where $g \rightarrow -2$, i.e. very close to the transition to the lamellar phase, the spinodal and the binodal nearly coincide. The incipient instability of the structured fluid to the lamellar phase appears to catalyse the phase separation. The second change is even more dramatic. In contrast to a simple fluid mixture, here the most unstable fluctuation at the spinodal has finite wavelength and the maximum growth rate ω_p drops to zero with a finite and rather steep slope. Therefore the region in which nucleation process compete with spinodal

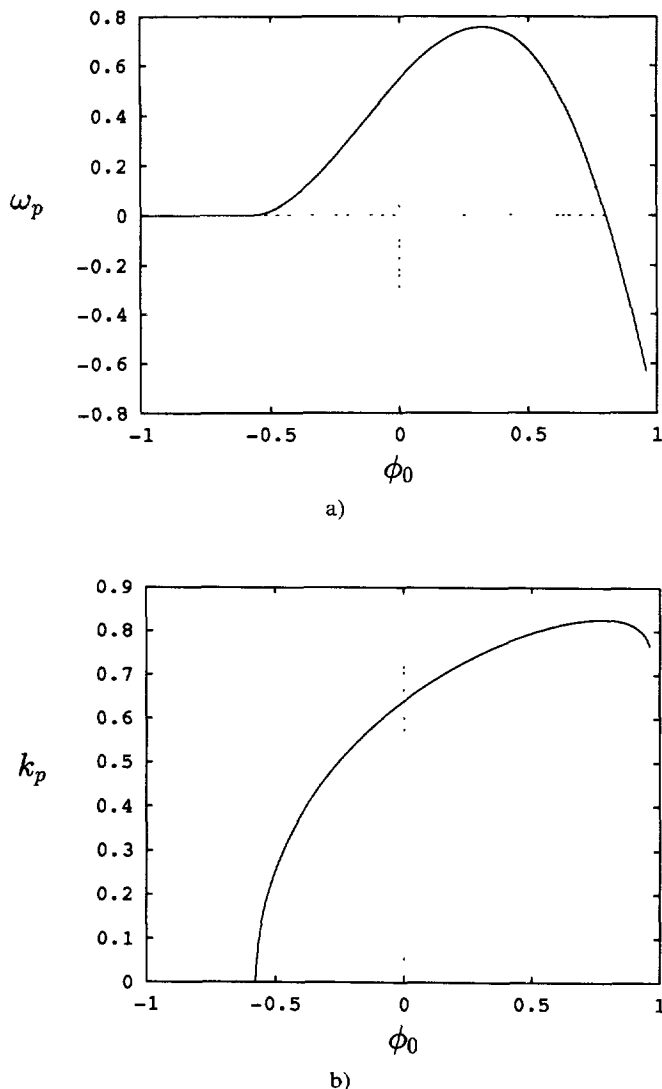


Fig. 1. — Cahn-Hilliard approximation : a) growth rate $\omega_p = \max_k [-1/\tau(k)]$ and b) wave vector k_p of the most unstable fluctuation after a quench into the two-phase region with $\bar{q} = 1.7$, vs order parameter ϕ_0 .

decomposition should be much smaller and the spinodal should be better defined. As a consequence, the concept of a spinodal is useful even beyond the Cahn-Hilliard-Cook approximation in a complex fluid and it may be possible to locate it experimentally.

We now proceed to the full treatment, considering model (2) with $\bar{q} = 1.7$ and accounting for fluctuations as described in the previous section and in the appendix.

Figure 2 shows the structure function at different times for both spinodals, on the normal-fluid side ($\phi_{sp} = -0.58$) and on the complex-fluid side ($\phi_{sp} = 0.8$). In both cases, the structure function develops a peak ; it grows faster on the complex-fluid side of the phase diagram, and the corresponding wavevector k changes less in time. Thus, the system on the

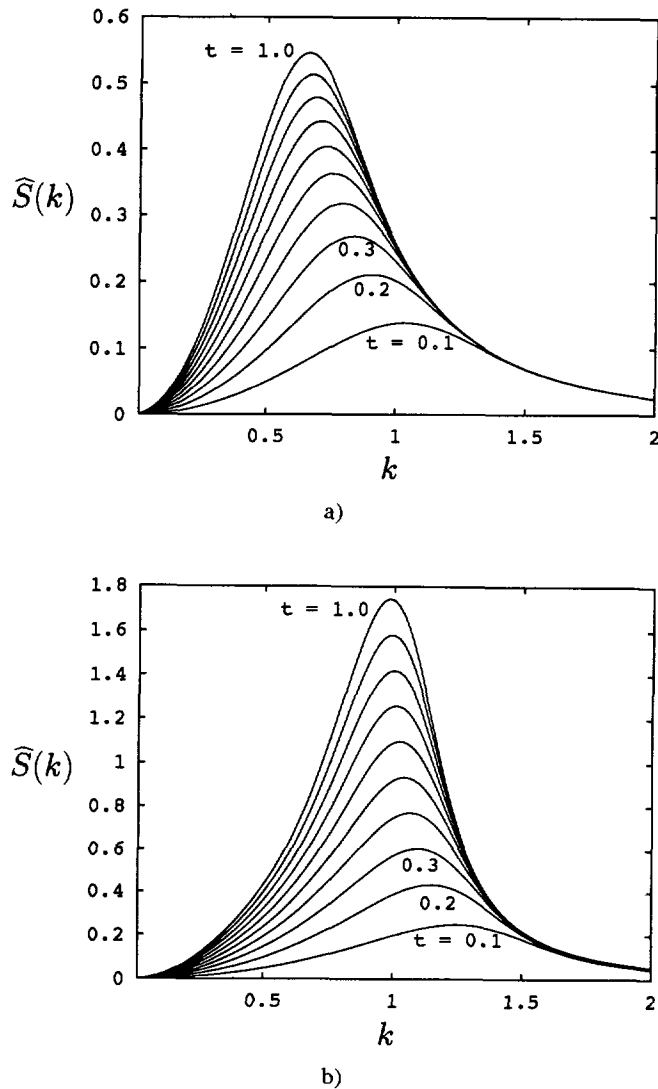


Fig. 2. — Structure function $\widehat{S}(k)$ for different times between $t = 0.1$ and $t = 1$. a) at $\phi_0 = -0.58$, b) at $\phi_0 = 0.8$.

complex-fluid side is driven towards a lamellar-phase-like intermediate structure which mediates the phase separation : spinodal decomposition in a complex fluid has qualitatively a very different character than in a simple fluid.

Nevertheless, if one just looks at $\widehat{S}(k)$, locating the spinodal on the complex-fluid side remains as difficult as on the simple-fluid side. The structure functions change only slightly as ϕ_0 crosses the spinodal. It proves useful to consider the time derivative $\partial_t \widehat{S}$ instead. While nothing special appears to happen at the spinodal on the simple-fluid side (Fig. 3), its behavior changes qualitatively as the spinodal on the complex-fluid side is passed : in the nucleation regime, $\partial_t \widehat{S}$ decreases in time, in the spinodal regime, it decreases first and then increases again. These two regimes are clearly distinct (Fig. 4).

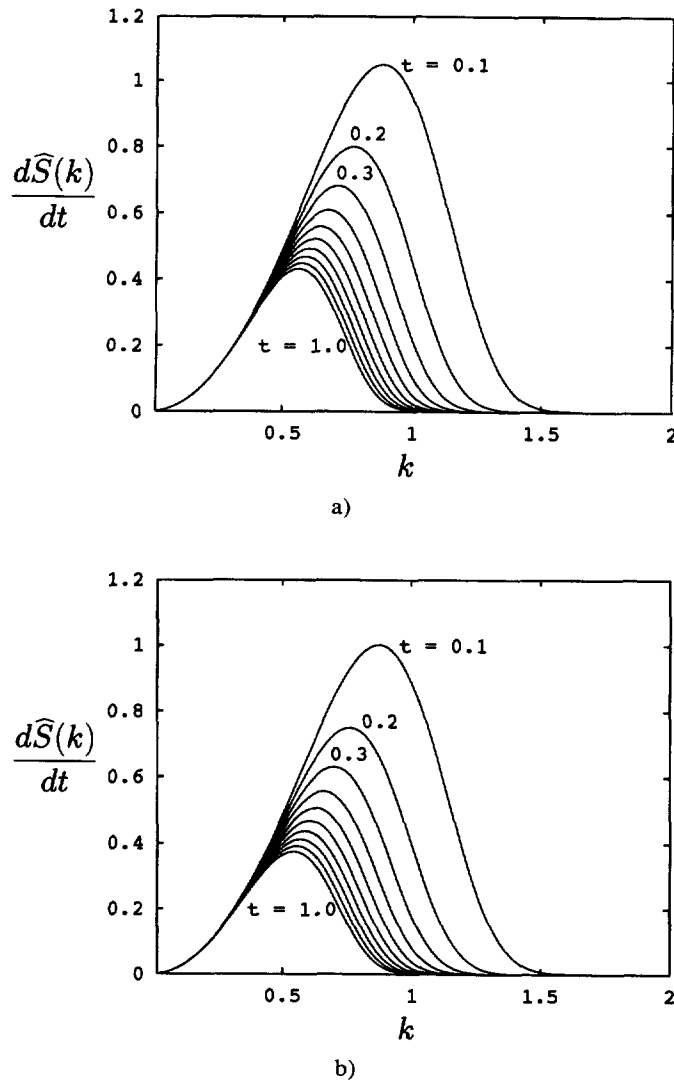


Fig. 3. — Time derivative of the structure function for different times a) at $\phi_0 = -0.55$, b) at $\phi_0 = -0.6$.

Another useful quantity to examine is the logarithmic derivative of the structure function $\partial_t \hat{S} / \hat{S}$. In the Cahn-Hilliard-Cook approximation (11), it is simply given by

$$\frac{\partial_t \hat{S}(\mathbf{k})}{\hat{S}(\mathbf{k})} = \frac{1}{t} h\left(\frac{t}{\tau(\mathbf{k})}\right) \quad (14)$$

with $h(x) \xrightarrow{x \rightarrow 0} 1 - \frac{1}{2}x + \frac{1}{12}x^2 - \dots$. Hence, $[\partial_t \hat{S}(\mathbf{k}) / \hat{S}(\mathbf{k}) - 1/t]$ roughly gives the characteristic growth rate, $-1/\tau(\mathbf{k})$, of a mode \mathbf{k} . Figure 5 shows the maximum value of this quantity for different times as a function of ϕ . One easily identifies a spinodal on the complex-fluid side of the phase diagram. On the simple-fluid side, the exact location is still difficult to determine,

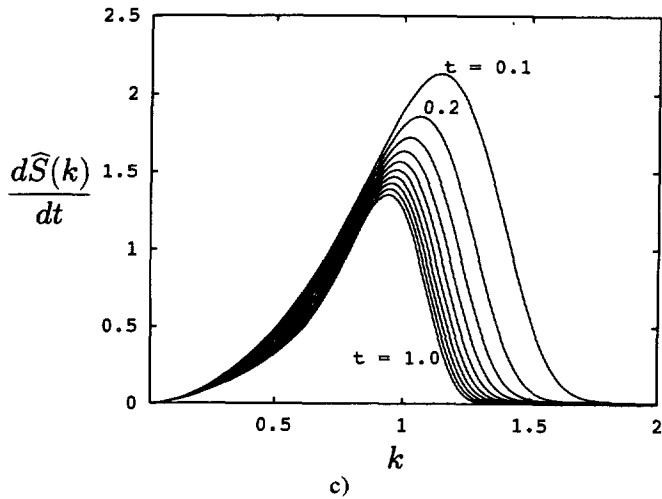
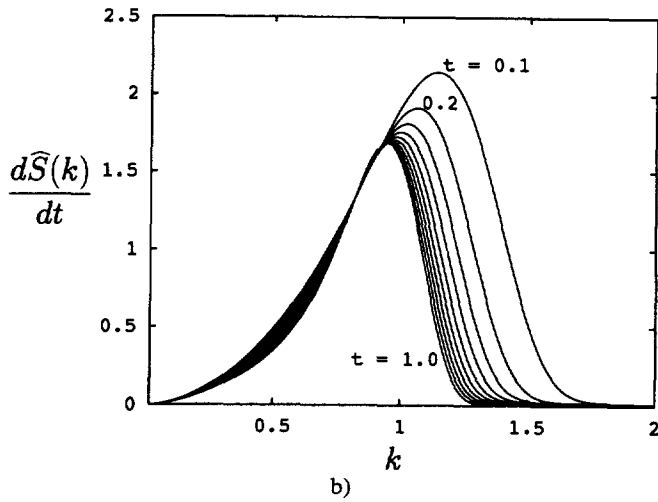
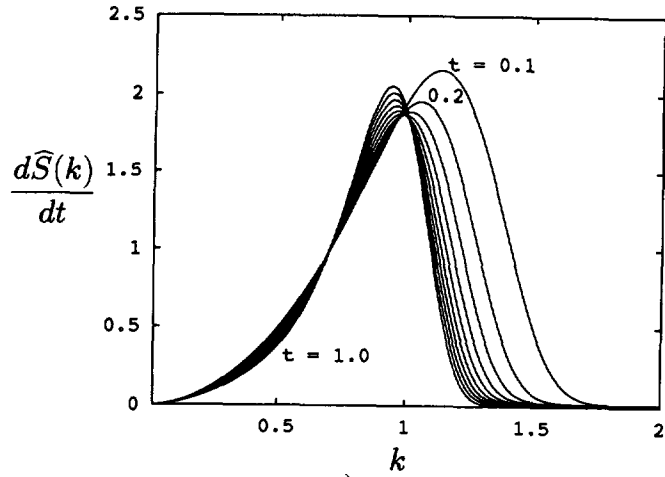


Fig. 4. — Time derivative of the structure function at different times a) at $\phi_0 = 0.75$, b) at $\phi_0 = 0.8$, c) at $\phi_0 = 0.85$.

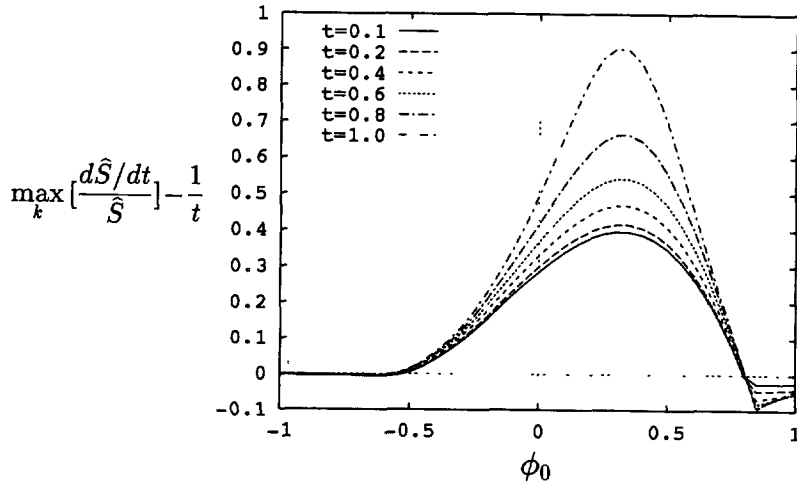


Fig. 5. — $\left\{ \max_k \left[\frac{d\hat{S}}{dt} / \hat{S} \right] - 1/t \right\}$ vs. ϕ_0 at different times.

especially since the curves are expected to smear out due to nucleation events. We note that figure 5 is strikingly similar to figure 1: the main features of spinodal decomposition in complex fluids are already evident in the Cahn-Hilliard-Cook approximation. The quantitative behavior however changes as one includes fluctuations since $\partial_r \hat{S}(\mathbf{k})$ ceases to behave exponentially in time as predicted by the approximation. On the complex-fluid side of the phase diagram, it may even be nonmonotonic in time, as is evident e.g. in figure 4a.

5. Summary and discussion.

In the present work we have discussed early-stage spinodal decomposition within a simple model for a complex fluid. We have studied the time evolution of the structure function $\hat{S}(\mathbf{k})$ in mean-field (Cahn-Hilliard-Cook) theory and included fluctuations in a Langer — Bar-on — Miller type approximation. Our main results can be summarized as follows:

i) the presence of internal structure in the fluid shrinks the metastability region of the phase diagram. In fact, for an ideally strong amphiphile the spinodal approaches the binodal, leaving no nucleation regime at all;

ii) in contrast to simple fluids, the unstable fluctuations at the spinodal have a definite wavelength;

iii) in contrast to simple fluids, in complex fluids the maximum growth rate (the maximum of $\partial_r \hat{S} / \hat{S} - 1/t$) drops to zero at the spinodal with a finite slope, making the spinodal considerably more sharply defined than in a simple fluid. This should be found in experiments as well as in simulations;

iv) in general, the results of the simple Gaussian theory (Cahn-Hilliard-Cook) are in remarkable qualitative agreement with the nonlinear theory. However, the linearized theory does not predict the non-monotonous growth behavior of $\partial_r \hat{S}$ which can be found on the complex-fluid side of the phase diagram.

We explain the second point in somewhat more detail. While the unstable fluctuations in a simple fluid have all wavelengths up to a minimum value, we find that in a complex fluid there

is a restriction of these modes to a band of finite wavelength, with this band narrowing down to zero width as the classical spinodal curve is reached. Motivated by this we tentatively like to interpret our results in terms of an intermediate state which mediates the phase separation on the complex fluid side. As is reflected by its internal structure, the complex fluid shows some affinity to a modulated, i.e. lamellar phase. Deeper in the two-phase coexistence region the homogeneous phase becomes increasingly unstable to both phase separation and to the formation of a modulated structure. On a short time-scale the short-wavelength local ordering wins the competition with the long-wavelength phase separation. In some respects this is similar to the phenomenon of simultaneous ordering and phase separation commonly found in metallic alloys [19]. In the situation we study, however, the spinodal decomposition leads to two homogeneous phases. To be more specific : local ordering to some extent already takes place beyond the binodal, in the stable complex fluid, since the internal structure has to establish itself. However, the instability of fluctuations with ordering wavevector points towards a much stronger ordering tendency within the spinodal, in the unstable region. Thus, the local order has to decrease again in the later stages of phase separation. Unfortunately, due to our approximations these are not within reach of our study.

To conclude, we have shown that the internal structure in a complex fluid gives rise to a number of new, interesting effects in spinodal decomposition. We expect that it would likewise affect the nucleation and the decomposition at intermediate stages. A very complex demixing behavior has for example recently been reported in thin copolymer films [7].

Acknowledgements.

We wish to acknowledge Michael Schick for suggesting the problem and for valuable discussions. F. S. has received financial support from the Deutsche Forschungsgemeinschaft. R. B. wishes to thank the University of Washington for its hospitality during a stay and acknowledges support by the DFG under SFB 237. This work was also supported in part by Grant No. DMR9220733 of the NSF.

Appendix.

We give the result for the set of coupled equations for the structure function $\hat{S}(\mathbf{k})$ (Eq. (8)) and the one-point distribution functional $\rho^{(1)}$ (Eq. (5)) :

$$\partial_t \hat{S}(\mathbf{k}) = -2 \lambda k^2 \left\{ \hat{S}(\mathbf{k}) A(\mathbf{k}) + a^3 \left(\frac{1}{2 \pi^2} \int_0^{k_m} dq q^4 \hat{S}(\mathbf{q}) - \Delta_2 \langle u^2 \rangle \right) (\beta + 2 \alpha) + a^3 \langle u^2 \rangle k^2 \alpha \right\} + 2 \lambda k_B T k^2, \quad (15)$$

$$\partial_t \rho^{(1)}(u) = \lambda \frac{\partial}{\partial u} \left[\rho^{(1)}(u) F(u) + k_B T \frac{\Delta_2}{a^3} \frac{\partial \rho^{(1)}}{\partial u} \right], \quad (16)$$

where

$$\begin{aligned} F(u) = & u \cdot \frac{1}{2 \pi^2} \int_0^{k_{\max}} dk \frac{\hat{S}(\mathbf{k})}{\langle u^2 \rangle} k^4 A(\mathbf{k}) \\ & + \frac{1}{2 \pi^2} \int_0^{k_{\max}} dk \frac{\hat{S}(\mathbf{k})}{\langle u^2 \rangle} k^4 \Delta_2 [2 b(u) + u \mathcal{L}_g(u)] \\ & - \Delta_2^2 u (\beta + \alpha) + (\Delta_4 - \Delta_2^2) b(u) + \Delta_4 \mathcal{L}_G(u) + \Delta_2 \mathcal{L}_{\partial f / \partial u}(u) \end{aligned}$$

and

$$A(\mathbf{k}) = 2ck^4 + k^2 \left[\frac{\langle uG \rangle}{\langle u^2 \rangle} + \langle g \rangle \right] + \Delta_2(\beta + \alpha) + \frac{\langle u(\partial f/\partial u) \rangle}{\langle u^2 \rangle}$$

with

$$\begin{aligned} \alpha &= \langle ug \rangle \langle u^3 \rangle / \langle u^2 \rangle^2 & dG(\phi)/d\phi &= g(\phi) \\ \beta &= \langle (u^2 \mathcal{L}_g(u)) \rangle / \langle u^2 \rangle & \Delta_2 &= \frac{3}{5} k_{\max}^2 \\ b(u) &= \langle ug \rangle (u^2 / \langle u^2 \rangle - 1) & \Delta_4 &= \frac{3}{7} k_{\max}^4 \\ \mathcal{L}_f(u) &= f(u) - \langle f(u) \rangle - u \langle uf(u) \rangle / \langle u^2 \rangle . \end{aligned}$$

In the derivation of the equations, the sum over wave vectors $\Sigma_{\mathbf{k}}$ has everywhere been replaced by the integral $(2\pi^2)^{-1} \int_0^{k_{\max}} dk k^2$; $k_{\max} = (6\pi^2/a^3)^{1/3}$ is an upper cutoff in which a is a coarse-graining length, a free parameter of the theory, chosen to be of the order of the bulk correlation length.

Instead of solving the partial equation (16) directly, we chose to consider the set of ordinary equations for the higher moments $\langle u^n \rangle$, which can be derived from them. In order to control the arbitrariness involved in the choice of the coarse-graining length a and the number of moments included, we varied both and studied the effect on the results. Not surprisingly, the values for the higher moments depend on a . The structure function itself remains independent of a until the higher moments become large compared to the first, and the calculation breaks down. This happens the sooner, the smaller one chooses the value of a . On the other hand a has to be small enough so that the structures developing during spinodal decomposition are apparent. We found $k_{\max} = 2.0$ to be a reasonable choice for our model. Furthermore, the inclusion of eleven moments was found to be sufficient, since results vary only very little beyond this value.

References

- [1] For reviews see, e.g., Langer J. S., *Systems Far From Equilibrium*, L. Garrido Ed., Lecture Notes in Physics 132 (Springer Verlag, Heidelberg, 1980, p. 12 ; Binder K., *ibid.*, (1980) p. 76 ; Gunton J. D., San Miguel M., Sahni P.S., *Phase Transitions and Critical Phenomena*, C. Domb, J. Lebowitz Eds., Vol. 8 (Academic Press, London) 1983, p. 267 ; Binder K., *Rep. Prog. Phys.* **50** (1987) 783.
- [2] Cahn J. W., Hilliard J. E., *J. Chem. Phys.* **28** (1958) 258 and **31** (1959) 688 ; Cahn J.W., *J. Chem. Phys.* **30** (1959) 1121 and **42** (1965) 93.
- [3] Becker R., Döring W., *Ann. Physik* **5** (1935) 719 ; Zel'dovich Y. B., *Zh. Eksp. Teor. Fiz.* **77** (1979) 1417.
- [4] Gerold V., Kistorz G., *J. Appl. Cryst.* **11** (1978) 376.
- [5] Siggia E. D., *Phys. Rev. A* **20** (1979) 595.
- [6] Hashimoto T., Kumaiki J., Kawai H., *Macromolecules* **16** (1983) 641 ; Snyder H. L., Meakin P., Reich S., *Macromolecules* **16** (1983) 757.
- [7] Maaloum M., Ausserre D., Chatenay D., Gallot Y., *Phys. Rev. Lett.* **70** (1993) 2577.
- [8] Beysens D., Perrot F., Guenoun P., *Phys. Rev. A* **32** (1985) 1818 ; Jayalakshmi Y., Khalil B., Beysens D., *Phys. Rev. Lett.* **69** (1992) 3088.
- [9] Wilcoxon J. P., Kaler E. W., *J. Chem. Phys.* **86** (1987) 4684.

- [10] Teubner M., Strey R., *J. Chem. Phys.* **87** (1987) 3195.
- [11] See e.g. *Physics of Amphiphilic Layers*, J. Meunier, D. Langevin and N. Boccaro Eds., Springer Proceedings in Physics, Vol. **21** (Springer, Berlin, 1987).
- [12] Levin Y., Mundy C. J., Dawson K. A., *Physica A* **196** (1993) 173.
- [13] Laradji M., Guo G., Grant M., Zuckermann M. J., *J. Phys. A* **24** (1991) L629 ; *J. Phys. . Condens. Matter* **4** (1992) 6715 ;
Yao J. H., Laradji M., *Phys Rev. E* **47** (1993) 2695.
- [14] Gompper G., Schick M., to appear in *Phase Transitions and Critical Phenomena*, C. Domb, J. Lebowitz Eds.
- [15] Note that in this treatment the total surfactant concentration is not conserved :

$$\langle \psi \rangle = - \left\langle \frac{\partial \mathcal{F}}{\partial \mu} \right\rangle = \langle [\mu + \ell (\nabla \phi)^2 - v_1(\phi)]/v_2 \rangle$$
. In order to keep $\langle \psi \rangle$ constant, the chemical potential μ has to be adjusted continuously and one gets time dependent functions g and f . We will neglect this time dependence from here on.
- [16] Gompper G., Schick M., *Phys. Rev. Lett.* **65** (1990) 1116.
- [17] Langer J. S., Bar-on M., Miller H. D., *Phys. Rev. A* **11** (1975) 1417.
- [18] Cook H. E., *Acta Metall.* **18** (1970) 297.
- [19] Allen S. M., Cahn J. W., *Acta Metall.* **24** (1976) 425 ;
Radmilovich M., Fox A. G., Thomas G., *Acta Metall.* **37** (1989) 2385 ;
Chen L. Q., Khachatryan A. G., *Acta Metall.* **39** (1991) 2533.